FUDMA Journal of Sciences (FJS)
ISSN online: 2616-1370
ISSN print: 2645 - 2944
Vol. 8 No. 3, June, 2024, pp 201 - 213
DOI: https://doi.org/10.33003/fjs-2024-0803-2499

ONE-STEP CENTRAL COMPOSITE-DESIGNED OPTIMIZATION FOR LEAD (II) IONS ADSORPTION ONTO PRISTINE AND ACID-MODIFIED ORANGE-PEELS FROM SIMULATED WASTEWATER

***[1]Sadiq Sani, [2]Haruna Abdullahi and [1]Abubakar Mansir Mazoji**

[1]Department of Chemistry, Federal University of Dutsin-Ma, P.M.B. 5001, Dutsinma, Nigeria
[2]Department of Industrial Chemistry, Federal University of Dutsin-Ma, P.M.B. 5001, Dutsin-Ma,

*Corresponding authors' email: sadiqsani123@gmail.com

ABSTRACT

A one-step response surface methodology using a half face-centred central composite design was utilized to optimize the efficiency of pristine orange peels powder (POPP) and acid-modified orange peels powder (AMPP) as adsorbents for lead (II) ions removal from aqueous solution with contact time (X_1), adsorption temperature (X_2), adsorbent dosage (X_3), adsorbate concentration (X_4) and adsorbate pH (X_5) as the independent variables. Analysis of variance (ANOVA) for the models indicated X_1, X_3, X_1X_3, X_2X_4, X_2X_5, X_1^2, X_3^2, and X_5^2 to have significant effects ($p < 0.05$) on the lead (II) ions removal efficiencies onto both adsorbents, while X_1X_2, X_1X_3, X_1X_5, X_2X_3, X_3X_4, X_3X_5, X_4X_5, X_2^2 and X_4^2 exhibited no significant effects ($p > 0.05$). The F-values approximately doubled from values in the initial models (POPP, F = 9.06; AMPP, F = 8.77) to those in the reduced models (POPP, F = 18.37; AMPP, F = 17.46) with low probability ($p < 0.0001$). Under optimum conditions, predicted values of the removal efficiencies (POPP, 100.7%; AMPP, 100.0%) strongly agreed with the mean confirmatory values from experiments (POPP 99.8 ± 0.9%; AMPP, 98.1 ± 0.9%). POPP and AMPP are potential low-cost adsorbents with high efficiency for lead (II) ions removal from aqueous solution.

Keywords: Adsorption efficiency, ANOVA, Central composite design, Lead (II) ions, Orange peels, Response surface methodology

INTRODUCTION

Large amounts of untreated industrial effluents loaded with heavy metals from the manufacturing activities are regularly discharged into adjacent water bodies (Ali *et al.*, 2019; Iloms *et al.*, 2020). Heavy metal ions are commonly regarded as primary contaminants classified as toxic, non-biodegradable, mutagenic, carcinogenic and mobile chemical pollutants that persist in the environment (Asiminicesei *et al.*, 2020; Gopinath *et al.*, 2020). One of the extremely toxic heavy metal ions known is lead (II) ions (Pb^{2+}) capable of causing several human health problems and environmental issues even at very low concentrations levels in water (El-Naggar *et al.*, 2019; Liu & Ma, 2020). The main sources of water contamination by Pb^{2+} are the release of completely untreated or partially treated effluents from industrial production of Lead-acid battery, paint, pigment, glass and, heavy chemical, pesticides metallurgical processes, electroplating, plastics, fertiliser processing, and mining activities (Li *et al.*, 2008; Tunali Akar *et al.*, 2012). The acceptable levels of Pb^{2+} concentration in water are 10 μgL^{-1} in line with the guidelines by the World Health Organization (World Health Organization, 2011). Ingestion of excess Pb^{2+} concentrations beyond the allowed threshold has been ascertained to cause human health issues including the defective central nervous system, mental retardation, memory loss, headache, gastrointestinal diseases, and kidneys failure (Gunarathne *et al.*, 2018). Adequate remediation of pollution due to Pb^{2+} in water is required to overcome the significant threat they potentially pose to the ecosystem.

Various methods such as electrochemical treatment (Raril & Manjunatha, 2020), hybrid flotation-membrane filtration (Blöcher *et al.*, 2003), chemical precipitation (J. Wu *et al.*, 2021), ion exchange (Ibrahim *et al.*, 2019), precipitation-flotation process (H. Wu *et al.*, 2021), electrocoagulation (Heffron *et al.*, 2016), forward osmosis (Soo *et al.*, 2020), and reverse osmosis (Petrinic *et al.*, 2015), have been used to remediate wastewater containing Pb^{2+}. The drawbacks to these approaches include high costs of implementation and electricity. Adsorption process using agricultural waste adsorbent has been ascertained to be highly viable due to its reproducibility, implementation cost-efficiency, relative simplicity, adsorbent abundance at low-cost, low sludge formation, and potential scalability for commercial applications (Ighalo & Adeniyi, 2020). Many fruits and vegetable wastes have been used as natural adsorbents for the removal of Pb (II) ions due to their biodegradable, resilience, low-cost, renewability, and richness surface functional groups (Moyo *et al.*, 2013; Ungureanu *et al.*, 2020). Different studies, such as pomelo (*Citrus grandis*) peel (Hameed *et al.*, 2008), waste lemon peels (Duru *et al.*, 2023), banana peels (Zhou, Chen, Feng, *et al.*, 2017; Zhou, Chen, Xi, *et al.*, 2017), residual tea leaves waste (Joshi *et al.*, 2020), orange peels xanthate (Ben Khalifa *et al.*, 2019), and cucumber peels (Basu *et al.*, 2017) have been carried out on the efficiency of biomass for Pb^{2+} removal.

Citrus fruit production for Nigeria was pegged at 4.07 million metric tons in 2018 (Knoema, 2018). The total global production of orange fruits stood at 53.72 million metric tons in 2016/2017 leading to the generation of huge quantities of solid wastes in the form of orange fruits peels (Ben Khalifa *et al.*, 2019). The practice of recovery and reuse of such waste materials in wastewater treatment ensures environmental sustainability through the clearing the orange peels solid waste and using it to reclaim of water resources via removal of heavy metal pollutants such as lead (II) ions.

In adsorption process optimization, experimental design and statistical analysis of the experimental outcomes are powerful tools used in the assessment of interactions among independent variable parameters, development of model equations for reliable prediction of the removal efficiency as well as optimize time and material resources. Only a few investigations have been reported on the one-step optimization of lead (II) ions removal onto both pristine and modified forms of orange fruit peels utilizing a one-step approach response surface design and optimization.

The present work aims to develop statistical models for optimizing the removal efficiencies of lead (II) ions by adsorption onto pristine orange fruit peels powder (POPP) and nitric acid-modified orange fruit peels powder (AMPP) under the optimum influence of select operational parameters (contact time, adsorbate pH, adsorbent dosage, adsorbate concentration and temperature) using a half face-centred central composite design (HFC-CCD) response surface methodology (RSM). The characterization of surface morphology and functional groups elucidations of these two adsorbents has been reported in our recent work (Sani *et al.*, 2019).

MATERIALS AND METHODS

Chemical reagents and adsorbents

Lead (II) nitrate ($Pb(NO_3)_2$) were purchased from Alfa Aesar, Karlsruhe, Germany. Sodium hydroxide (NaOH), hydrochloric acid (HCl) and nitric acid (HNO_3) were obtained from Fisher Chemical, Loughborough, United Kingdom. The entire chemical reagents were employed as received without any further purification.

Orange peels adsorbents and simulated adsorbate

Collection and preparation of the orange peels used as adsorbents samples were reported in our previous work (Sani *et al.*, 2019). Briefly, the pristine orange peels powder (POPP) was prepared from the crispy oven-dried peels by pulverization and sieving through a 1-mm mesh size sieve. The modified orange peels powder (AMPP) was prepared in accordance to Igwe *et al.* (2010) by soaking 25-g aliquots of the POPP in 0.3 M nitric acid (HNO_3) aqueous solution for 24 h, filtering out the supernatant from the mixture, and copiously washing the resulting paste of the solid residue with distilled water until the pH of the filtrate tested almost neutral (~ 7.0). The solid was then dried in air for 24 h at 25 °C followed by oven-drying for 14 h at 90 °C before being stored in an air-tight sample vessel for subsequent experimentations. Three levels of the simulated wastewater concentrations (10 mgL^{-1}, 255 mgL^{-1} and 500 mgL^{-1}) were prepared by diluting specific aliquots of a stock solution containing 1000 mgL^{-1} of the Pb (II) ions in separate volumetric flasks of appropriate capacities.

Response surface design matrix

A one-step optimization using a half face-centred central composite design (HFC-CCD) was used to study the impact of the operating conditions for lead ion adsorptive removal from an aqueous medium. Minitab 19.1 statistical software (Minitab®, 2019) was used for regression analysis of experimental data and to plot response surface while ANOVA was used to estimate the statistical parameters. The five independent variables of choice were A: contact time (X_1), B: adsorption temperature (X_2), C: adsorbent dosage (X_3), D: adsorbate concentration (X_4), and E: adsorbate pH (X_5). Each of the factors was represented as a set of three different normalized coded levels of −1, 0, +1 corresponding to the low, middle, and high values of the factors (where $-1 \leq X \leq +1$). The factors and their respective levels for the design matrix in actual and coded values are summarized in Table 1. The order of the runs was randomised to prevent systematic errors.

Table 1: Actual and coded levels of factors affecting Pb (II) ions adsorption onto the adsorbents

Predictor variables	Symbol	Predictor level		
		Low (−1)	*Middle (0)*	*High (+1)*
$\boldsymbol{X_1}$: Contact time (min)	A	30	90	150
$\boldsymbol{X_2}$: Adsorption temperature (K)	B	303	318	333
$\boldsymbol{X_3}$: Adsorbent dosage (g)	C	0.5	1	1.5
$\boldsymbol{X_4}$: Adsorbate concentration (mg/L)	D	10	255	500
$\boldsymbol{X_5}$: Adsorbate pH	E	3	6	9

The HFC-CCD generated has a design matrix of 32 total experimental runs, N (determined by Equation [1]) made up of 16 cubic points, six replicated centre points in the cube (N_0), and 10 axial points with no centre points in the axial direction. Systematic errors were eliminated by conducting the experimental sequence in the randomized run order. Analyses of the experimental results were carried out using response surface regression approach where the correlation between the adsorption parameters and Pb (II) removal efficiencies of the adsorbents was evaluated by fitting into the second-order polynomial in equation (Ibrahim *et al.*, 2019).

$$N = 2^{k-1} + 2k + N_0 \tag{1}$$

$$Y = \beta_o + \sum_{i=1}^{k} \beta_i x_i + \sum_{i=1}^{k} \beta_{ii} x_{ii}^2 + \sum_{i=1}^{k} \sum_{i \neq j=1}^{k} \beta_{ij} x_i x_j + \varepsilon \tag{2}$$

where Y is the Pb(II) ion removal efficiency, k represents the number independent variable parameters, β_0 is the intercept on the vertical axis representing a fixed removal efficiency at the design centre-point and β_i, β_{ii}, and β_{ij} are the constant coefficients for the linear, quadratic, and interaction terms of the model respectively. The terms x_i and x_j are the coded levels for independent variable parameters and ε is the total pure error. Pure error sum of squares was estimated through the inclusion of a total of six cubic centre points replicates as proposed by the design software. All the axial (or star) points are on the faces of the cube such that the distance of each axial point from the centre of the design matrix (α) is one based on evaluation from Equation (Heffron *et al.*, 2016).

$$\alpha = (2^{k-1})^{0.25} \tag{3}$$

Batch adsorption experiments

adsorption experiments were conducted using the batch process to optimize the removal efficiencies of Pb (II) ions from aqueous medium onto POPP and AMPP adsorbents following the HFC-CCD matrix. During a specific experimental run, 50 cm^3 of 255 mg/L Pb (II) ion solution at an adjusted pH of six (achieved by adding specific aliquots of 0.2 M HCl or 0.2 M NaOH solution) was added into a 250-cm^3 Erlenmeyer flask containing 0.50 g weight of POPP. The flask containing the mixture was transferred into a thermostatic hot water bath, heated to 318 K for 90 min, cooled to ambient temperature (298 K), followed by filtering through a Whatman No. 41 filter paper (20 µm pore size). The supernatant was then diluted to the mark in a 100-cm^3 volumetric flask and analysed for Pb (II) ions residual content using atomic absorption spectrophotometer (AA 6800, Shimadzu, Japan). Equation 4 was used to evaluate the efficiencies, Y_1 (%) and Y_2 (%), for the removal of Pb (II) ions from solution onto POPP.

$$Y(\%) = \frac{C_i - C_f}{C_i} \times 100 \qquad (4)$$

where Y (%) is the Pb (II) metal ions removal efficiency the adsorbent, C_i and C_f are the initial and residual concentrations of the ions in the simulated wastewater, respectively.

RESULTS AND DISCUSSIONS

Response surface regression model development and analysis

An HFC-CCD matrix of the 32 statistically designed experimental runs combining five independent variable parameters with the corresponding values of the experimentally observed Pb (II) ions removal efficiencies (Y_1, Y_2) and their predicted counterparts (Y_1', Y_2') for adsorption onto POPP and AMPP adsorbents are given in Table 2, respectively.

Table 2: Observed and predicted lead (II) ions removal efficiencies of the adsorbents in the randomized CCD matrix

Run	t (min)	T (K)	W (g)	M (mg/L)	pH	POPP		AMPP	
						Y_1 (%)	Y_1' (%)	Y_2 (%)	Y_2' (%)
1	90	318	0.5	255	6	91.4	92.5	89.7	90.8
2	90	318	1.0	255	6	86.7	86.3	85.0	84.7
3	150	333	0.5	500	3	93.5	93.6	91.8	91.9
4	90	333	1.0	255	6	88.1	86.1	86.9	84.6
5	30	303	0.5	10	9	91.2	90.7	89.5	89.0
6	90	303	1.0	255	6	84.5	88.2	83.0	87.0
7	90	318	1.0	255	3	94.5	94.6	92.8	93.1
8	150	318	1.0	255	6	85.7	85.6	84.3	84.2
9	30	303	1.5	10	3	83.4	83.2	82.5	82.3
10	90	318	1.0	255	6	87.4	86.3	85.7	84.7
11	30	303	0.5	500	3	92.0	91.2	90.3	89.4
12	150	303	0.5	10	3	100.4	100.4	99.7	99.7
13	30	303	1.5	500	9	79.1	78.1	77.4	76.5
14	90	318	1.0	255	9	91.8	93.4	90.4	91.7
15	30	333	1.5	500	3	83.8	83.8	82.6	82.6
16	30	333	1.5	10	9	76.3	76.7	74.6	75.1
17	150	303	1.5	500	3	101.1	100.5	100.0	99.4
18	150	333	1.5	500	9	98.3	98.3	96.8	96.9
19	150	333	0.5	10	9	93.5	94.0	91.8	92.4
20	90	318	1.0	255	6	86.2	86.3	84.5	84.7
21	30	333	0.5	500	9	93.2	92.9	91.5	91.3
22	30	333	0.5	10	3	82.9	83.4	81.2	81.7
23	150	303	0.5	500	9	94.1	93.3	92.9	92.1
24	30	318	1.0	255	6	72.6	74.4	70.9	72.7
25	150	333	1.5	10	3	92.9	93.7	91.7	92.5
26	90	318	1.0	500	6	81.5	84.8	79.8	83.0
27	90	318	1.5	255	6	88.1	88.8	86.9	87.4
28	90	318	1.0	255	6	85.2	86.3	83.5	84.7
29	90	318	1.0	255	6	91.8	86.3	90.6	84.7
30	90	318	1.0	255	6	87.2	86.3	85.6	84.7
31	90	318	1.0	10	6	84.6	83.0	82.9	81.4
32	150	303	1.5	10	9	95.9	95.8	95.1	95.0

Equations [4] and [5] represent the initial models for the actual efficiencies for the Pb (II) ions removal from the simulated wastewater onto the adsorbents. Response surface models of the second-order polynomials were employed in the estimation of the model coefficients, detection of interactions, determination of curvature, process optimization, and prediction of the appropriate models for the response validation.

$$\begin{aligned} Y_1(\%) = 635 &+ 0.420t - 2.83T - 61.4W - 0.1258M - 20.61(pH) - 0.001731t^2 + 0.00379T^2 \\ &+ 17.45W^2 - 0.000039M^2 + 0.859(pH)^2 - 0.000275tT + 0.0906tW \\ &- 0.000043tM - 0.00126t(pH) + 0.0542TW + 0.000472TM + 0.0343T(pH) \\ &+ 0.00452WM - 0.617W(pH) - 0.000248M(pH) \end{aligned} \qquad (5)$$

$$\begin{aligned} Y_2(\%) = 750 &+ 0.471t - 3.56T - 62.2W - 0.1348M - 20.82pH - 0.001735t^2 + 0.00491T^2 \\ &+ 17.78W^2 - 0.000042M^2 + 0.860(pH)^2 - 0.000422tT + 0.0893tW \\ &- 0.000046tM - 0.00103t(pH) + 0.0565TW + 0.000503TM + 0.0347T(pH) \\ &+ 0.00437WM - 0.646W(pH) - 0.000170M(pH) \end{aligned} \qquad (6)$$

Following the exclusion of several non-significant terms, the two initial models were transformed into their reduced forms represented by Equations (6) and (7). The improved second-order response surface models were similarly utilized in the estimation of the model coefficients, detection of interactions, determination of curvature, process optimization, and prediction of the appropriate model for effective validation of the responses.

$$Y_1(\%) = 245.7 + 0.3370t - 0.3964T - 43.1W - 0.1467M - 20.81pH - 0.001857t^2 + 15.64W^2 + 0.808(pH)^2 + 0.0906tW + 0.000472TM + 0.0343T(pH) \quad (7)$$

$$Y_2(\%) = 250.8 + 0.3397t - 0.416T - 43.7W - 0.1569M - 21.05(pH) - 0.001851t^2 + 16.11W^2 + 0.814(pH)^2 + 0.0893tW + 0.000503TM + 0.0347T(pH) \quad (8)$$

Analysis of variance (ANOVA) for the initial and reduced models

The most basic statistical method to reliably analyse the proportional effects of one or more predictor variable parameters on variations in the response variables, and effectively evaluate the quality of the fitted model of an experimental data is through using the analysis of variance (ANOVA). The statistical technique compartmentalized the total variation in the removal efficiencies concerning specific sources of variation for hypotheses test on the variable parameters used in the experimental data. Table 3 and Table 4 enumerate the outcomes of the ANOVA and F-test used to evaluate the statistical significance and the soundness of the developed initial quadratic models at 95% level of confidence ($\alpha = 0.05$).

Table 3: Analysis of Variance for Pb (II) ion removal onto POPP adsorbents based on the initial models

Source	DF	Contribution	Sum of Squares	Mean Squares	F-Value	P-Value
Model	20	94.28%	1259.51	62.975	9.06	0.000
X_1	1	42.29%	565.04	565.040	81.27	0.000
X_2	1	1.50%	20.01	20.013	2.88	0.118
X_3	1	4.56%	60.94	60.941	8.77	0.013
X_4	1	1.01%	13.45	13.451	1.93	0.192
X_5	1	0.51%	6.83	6.833	0.98	0.343
X_1^2	1	1.63%	21.74	95.609	13.75	0.003
X_2^2	1	6.56%	87.63	1.785	0.26	0.622
X_3^2	1	7.61%	101.70	46.817	6.73	0.025
X_4^2	1	0.06%	0.87	13.685	1.97	0.188
X_5^2	1	11.00%	146.92	146.917	21.13	0.001
X_1X_2	1	0.07%	0.98	0.980	0.14	0.714
X_1X_3	1	8.84%	118.16	118.157	16.99	0.002
X_1X_4	1	0.48%	6.35	6.350	0.91	0.360
X_1X_5	1	0.06%	0.82	0.819	0.12	0.738
X_2X_3	1	0.20%	2.64	2.641	0.38	0.550
X_2X_4	1	3.61%	48.23	48.233	6.94	0.023
X_2X_5	1	2.85%	38.07	38.069	5.48	0.039
X_3X_4	1	0.37%	4.91	4.906	0.71	0.419
X_3X_5	1	1.02%	13.69	13.690	1.97	0.188
X_4X_5	1	0.04%	0.53	0.533	0.08	0.787
Error	11	5.72%	76.48	6.953		
Lack-of-Fit	6	3.75%	50.13	8.354	1.58	0.315
Pure Error	5	1.97%	26.35	5.271		
Total	31	100.00%	1335.99			

Outcomes of ANOVA for the initial models (Table 3 and Table 4) indicate that two pure independent variable parameters (X_1, X_3), three interactive cross-product terms (X_1X_3, X_2X_4, X_2X_5) and three quadratic terms (X_1^2, X_3^2, X_5^2) were found to significantly affect ($p < 0.05$) the Pb (II) ions removal efficiencies onto both adsorbents. The conservative Fisher's F-test values for adsorption onto POPP ($F = 9.06$) and AMPP ($F = 8.77$) with very low probability values ($p < 0.0001$) demonstrates a high statistical significance of the regression models in depicting the actual relationship between the five independent variable parameters and the adsorption efficiencies of the adsorbents obtained from the experiments. Most of the interaction terms (X_1X_2, X_1X_3, X_1X_5, X_2X_3, X_3X_4, X_3X_5, X_4X_5) and some quadratic terms (X_2^2, X_4^2) in the initial models, however, exhibited inconsequential effects ($p > 0.05$) on the removal efficiencies, thus, necessitating their exclusion to improve the model.

Table 4: Analysis of Variance for Pb (II) ion removal onto AMPP adsorbent based on the initial models

Source	DF	Contribution	Sum of Squares	Mean Squares	F-Value	P-Value
Model	20	94.10%	1308.68	65.434	8.77	0.000
X_1	1	42.80%	595.24	595.240	79.82	0.000
X_2	1	1.84%	25.61	25.609	3.43	0.091
X_3	1	3.79%	52.67	52.668	7.06	0.022
X_4	1	0.79%	11.04	11.045	1.48	0.249
X_5	1	0.64%	8.88	8.876	1.19	0.299
X_1^2	1	1.84%	25.65	95.969	12.87	0.004
X_2^2	1	6.90%	96.00	3.005	0.40	0.539
X_3^2	1	7.42%	103.24	48.622	6.52	0.027
X_4^2	1	0.10%	1.33	15.379	2.06	0.179
X_5^2	1	10.60%	147.42	147.422	19.77	0.001
X_1X_2	1	0.17%	2.31	2.310	0.31	0.589
X_1X_3	1	8.25%	114.70	114.704	15.38	0.002
X_1X_4	1	0.53%	7.43	7.426	1.00	0.340
X_1X_5	1	0.04%	0.55	0.548	0.07	0.791
X_2X_3	1	0.21%	2.87	2.873	0.39	0.547
X_2X_4	1	3.94%	54.76	54.760	7.34	0.020
X_2X_5	1	2.81%	39.13	39.125	5.25	0.043
X_3X_4	1	0.33%	4.58	4.580	0.61	0.450
X_3X_5	1	1.08%	15.02	15.016	2.01	0.184
X_4X_5	1	0.02%	0.25	0.250	0.03	0.858
Error	11	5.90%	82.03	7.457		
Lack-of-Fit	6	3.69%	51.36	8.559	1.40	0.366
Pure Error	5	2.21%	30.67	6.134		
Total	31	100.00%	1390.71			

The outcomes of the ANOVA for the reduced models are presented in Table 5 and Table 6. Although all the second-order terms with trivial effects ($p > 0.05$) on the lead (II) removal efficiencies have been excluded from the reduced models, the three linear predictors with insignificant effects (X_2, X_4, X_5) are hierarchical terms of significant second-order terms ($X_2 X_4$, X_2X_5, X_5^2) retained in the models to conform with the hierarchy principle. In the reduced models, the Fisher's F values for adsorption onto POPP ($F = 18.37$) and AMPP ($F = 17.46$) increased to approximately twice their values in the initial models with very low probability values ($p < 0.0001$), demonstrating the high statistical significance of the reduced regression models in depicting the true relationship between the independent variable parameters and the adsorption efficiencies from the experiments. The lack-of-fit in both models remained insignificant ($p > 0.05$).

Table 5: Analysis of Variance for Pb (II) ion removal onto POPP adsorbents based on the reduced model

Source	DF	Contribution	Sum of Squares	Mean Squares	F-Value	P-Value
Model	11	90.99%	1215.66	110.514	18.37	0.000
X_1	1	42.29%	565.04	565.040	93.91	0.000
X_2	1	1.50%	20.01	20.013	3.33	0.083
X_3	1	4.56%	60.94	60.941	10.13	0.005
X_4	1	1.01%	13.45	13.451	2.24	0.150
X_5	1	0.51%	6.83	6.833	1.14	0.299
X_1^2	1	1.63%	21.74	127.536	21.20	0.000
X_3^2	1	12.88%	172.07	43.659	7.26	0.014
X_5^2	1	11.31%	151.11	151.113	25.12	0.000
X_1X_3	1	8.84%	118.16	118.157	19.64	0.000
X_2X_4	1	3.61%	48.23	48.233	8.02	0.010
X_2X_5	1	2.85%	38.07	38.069	6.33	0.021
Error	20	9.01%	120.33	6.017		
Lack-of-Fit	15	7.03%	93.98	6.265	1.19	0.459
Pure Error	5	1.97%	26.35	5.271		
Total	31	100.00%	1335.99			

Table 6: Analysis of Variance for Pb (II) ion removal onto AMPP adsorbent based on the reduced model

Source	DF	Contribution	Sum of Squares	Mean Squares	F-Value	P-Value
Model	11	90.57%	1259.57	114.506	17.46	0.000
X_1	1	42.80%	595.24	595.240	90.78	0.000
X_2	1	1.84%	25.61	25.609	3.91	0.062
X_3	1	3.79%	52.67	52.668	8.03	0.010
X_4	1	0.79%	11.04	11.045	1.68	0.209
X_5	1	0.64%	8.88	8.876	1.35	0.258
X_1^2	1	1.84%	25.65	126.711	19.33	0.000
X_3^2	1	12.86%	178.83	46.303	7.06	0.015
X_5^2	1	11.01%	153.06	153.057	23.34	0.000
X_1X_3	1	8.25%	114.70	114.704	17.49	0.000
X_2X_4	1	3.94%	54.76	54.760	8.35	0.009
X_2X_5	1	2.81%	39.13	39.125	5.97	0.024
Error	20	9.43%	131.14	6.557		
Lack-of-Fit	15	7.22%	100.46	6.698	1.09	0.503
Pure Error	5	2.21%	30.67	6.134		
Total	31	100.00%	1390.71			

The fit quality assessments of the initial and reduced quadratic polynomial models were carried out using the values of the coefficients of determination (R^2), and adjusted R^2 (Adj. R^2). Summary of the regression statistic of the two models for Pb (II) ions removal onto the adsorbents is presented in Table 7. Values of the determination coefficient for the lead (II) ions removal onto both POPP and AMPP adsorbents indicated that both models could account for 94% of total variations in the removal efficiencies ($R^2 = 0.94$) from the experimental data and unable of elucidating only 6.00% of the total variations. The adjusted R^2 values for removal onto POPP (Adj. $R^2 = 0.84$) and onto AMPP (Adj. $R^2 = 0.83$) agree with the R^2 values for the initial models, suggesting that the initial regression models explain 84% and 83% of the total variations in adjusted to the five independent variable parameters in the model relative to the 32 experimental runs in the design. The initial models, however, have no predictive capabilities for the Pb (II) ions removal efficiency onto the adsorbents as evident in the nought percentage value of their prediction R^2 (pred-R^2) values and very high values of the prediction error sum of squares (PRESS) of 3395.53 for removal onto POPP and 3590.98 onto AMPP. This trend was occasioned by the presence of a substantial number of non-significant terms ($p > 0.05$) in the model, hampering the prediction ability by lowering the signal-to-noise ratio in the models. Both models exhibited an insignificant lack-of-fit ($p > 0.05$), indicating that the models fit the experimental data well.

Sequel to the exclusion of the nine second-order terms with insignificant effects on the responses, the predictive ability of the two models improved significantly. PRESS in the reduced models decreased substantially to 12 times less than the values in the initial models, whereas the R^2-pred values improved from their nought values to 0.80 for removal onto POPP and 0.79 onto AMPP. Thus, the strong correlation between the R^2-pred and R^2 values demonstrated good agreement between the experimentally observed and predicted removal efficiencies onto both adsorbents in the reduced models.

Table 7: Regression statistic of initial and reduced models for Pb (II) ions adsorption onto the adsorbents

Regression statistic	Initial Model		Reduced Model	
	POPP	***AMPP***	***POPP***	***AMPP***
S	2.64	2.73	2.45	2.56
R-sq	0.94	0.94	0.91	0.91
R-sq(adj)	0.84	0.83	0.86	0.85
PRESS	3395.53	3590.98	266.51	289.87
R-sq(pred)	0.00	0.00	0.80	0.79
AICc	275.14	277.38	179.42	182.17
BIC	194.94	197.18	178.25	181.00

Student's t-tests were used in the analyses of the statistical results to determine the significance of the regression coefficients in the developed initial and reduced models as well as utilized their corresponding P-values as a tool to determining the significance of the independent variable parameters during the adsorption process. The regression coefficients, T-values, P-values for all first-order and second-order (quadratic and interaction) effects of the independent variable parameters from the initial and reduced models for adsorption onto both adsorbents are enumerated in Table 8 and Table 9 respectively.

Table 8: Estimated regression coefficients of the initial model and their significance

	Initial Y_1 model for removal onto POPP			**Initial Y_2 model for removal onto AMPP**		
Coefficient	***Value***	***T-Value***	***P-Value***	***Value***	***T-Value***	***P-Value***
β_0	86.262	114.47	0.000	84.686	108.52	0.000
β_1	5.603	9.01	0.000	5.751	8.93	0.000
β_2	-1.054	-1.70	0.118	-1.193	-1.85	0.091
β_3	-1.840	-2.96	0.013	-1.711	-2.66	0.022
β_4	0.864	1.39	0.192	0.783	1.22	0.249
β_5	-0.616	-0.99	0.343	-0.702	-1.09	0.299
β_{11}	-6.23	-3.71	0.003	-6.24	-3.59	0.004
β_{22}	0.85	0.51	0.622	1.11	0.63	0.539
β_{33}	4.36	2.59	0.025	4.45	2.55	0.027
β_{44}	-2.36	-1.40	0.188	-2.50	-1.44	0.179
β_{55}	7.73	4.60	0.001	7.74	4.45	0.001
β_{12}	-0.248	-0.38	0.714	-0.380	-0.56	0.589
β_{13}	2.718	4.12	0.002	2.677	3.92	0.002
β_{14}	-0.630	-0.96	0.360	-0.681	-1.00	0.340
β_{15}	-0.226	-0.34	0.738	-0.185	-0.27	0.791
β_{23}	0.406	0.62	0.550	0.424	0.62	0.547
β_{24}	1.736	2.63	0.023	1.850	2.71	0.020
β_{25}	1.542	2.34	0.039	1.564	2.29	0.043
β_{34}	0.554	0.84	0.419	0.535	0.78	0.450
β_{35}	-0.925	-1.40	0.188	-0.969	-1.42	0.184
β_{45}	-0.183	-0.28	0.787	-0.125	-0.18	0.858

Table 9: Estimated regression coefficients of the reduced model and their significance

	Reduced Y_1 model for removal onto POPP			**Reduced Y_2 model for removal onto AMPP**		
Coefficient	***Value***	***T-Value***	***P-Value***	***Value***	***T-Value***	***P-Value***
β_0	84.606	117.10	0.000	86.175	124.51	0.000
β_1	5.751	9.53	0.000	5.603	9.69	0.000
β_2	-1.193	-1.98	0.062	-1.054	-1.82	0.083
β_3	-1.711	-2.83	0.010	-1.840	-3.18	0.005
β_4	0.783	1.30	0.209	0.864	1.50	0.150
β_5	-0.702	-1.16	0.258	-0.616	-1.07	0.299
β_{11}	-6.66	-4.40	0.000	-6.68	-4.60	0.000
β_{22}	4.03	2.66	0.015	3.91	2.69	0.014
β_{55}	7.32	4.83	0.000	7.28	5.01	0.000
β_{13}	2.678	4.18	0.000	2.718	4.43	0.000
β_{24}	1.850	2.89	0.009	1.736	2.83	0.010
β_{25}	1.564	2.44	0.024	1.542	2.52	0.021

The null hypothesis (H_0) is that the regression coefficients of the two models and their corresponding linear, quadratic and interaction terms do not affect the adsorption efficiencies for removal of Pb (II) ions from the simulated wastewater onto the adsorbents. Whereas the alternative hypothesis (H_1) stated that the regression coefficients affect the adsorption efficiencies. In the initial models (Table 8), the absolute t-values for three linear coefficients (β_0, β_1, β_3), three quadratic coefficients (β_{11}, β_{33}, β_{55}) and three interaction coefficients (β_{13}, β_{24}, β_{25}) are greater than the critical t-value ($t_{\alpha/2,26} = 2.056$), leading to the rejection of the H_0 and acceptance of the H_1. for all other second-order regression coefficients with the absolute t-values less than the critical t-value (β_{22}, β_{44}, β_{12}, β_{14}, β_{15}, β_{23}, β_{34}, β_{35}, β_{45}) the H_0 was accepted, followed by their elimination from the initial model to reconstruct the new reduced model with more accurate regression coefficients (Table **9**). Although three of the linear coefficients (β_2, β_4, β_5) have absolute t-values less than the critical t-value in the reduced model, they must be included because they resulted from the non-significant terms in the design with significant second-order effects to maintain hierarchy in the reduced models.

Diagnostic quality charts

The diagnostic quality charts in Figure 1 and Figure 2 corroborate the statistical outcome of the analyses of variance for the reduced models. Normal probability plot of the effect plots (illustrated in Figure 1(a) and Figure 2(a)) determines the direction in addition to the importance and magnitude of the effects of independent variables levels on the Pb (II) ions removal efficiency onto the adsorbents. On both adsorbents, all the eight variable terms with statistically significant effects at $\alpha = 0.05$ on the plot are lying further away from the reference line along which the factors have zero effect on the response values. Whereas the X_1^2 and X_3 exhibit a negative standardized effect on the response decreasing the removal efficiency onto both adsorbents when increased from a low level to a high one, the terms X_1, X_5^2, X_1X_3, X_2X_4, X_3^2, and X_2X_5 have positive effect increasing the removal efficiency when they are increased.

The Pareto charts illustrated in Figure 1(b) and Figure 2(b) were employed to determine the magnitude and the importance of the effects independent variables on Pb (II) removal onto the adsorbents. bars that cross the reference line at 2.09 on the chart have statistically significant effects on the responses. the bars also present the decreasing order of significance to be $X_1 > X_5^2 > X_1^2 > X_1X_3 > X_3 > X_2X_4 > X_3^2 > X_2X_5$ and $X_1 > X_5^2 > X_1^2 > X_1X_3 > X_2X_4 > X_3 > X_3^2 > X_2X_5$ with the contact time as the most important independent parameter in each case for adsorption onto POPP and AMPP adsorbent, respectively. These factors are statistically significant at the 0.05 level with the current model terms.

Figure 1(c) and Figure 2(c) illustrate the normal probability plots of the two reduced models. The Anderson-Darling statistic (AD) of 0.261 and 0.240 with probabilities greater than 0.20 for removal onto POPP ($p > 0.684$) and AMPP ($p > 0.758$) that indicated that there is strong statistical evidence that the data are normally distributed, respectively.

Plots of residuals versus fitted response values (as illustrated in Figure 1(d) and Figure 2(d)) produced a distribution of points scattered randomly both below and above the line of zero-residual without any identifiable trend. This verifies the assumption that the residuals of the predicted adsorption efficiencies have constant variances and are also randomly distributed for removal onto both adsorbents.

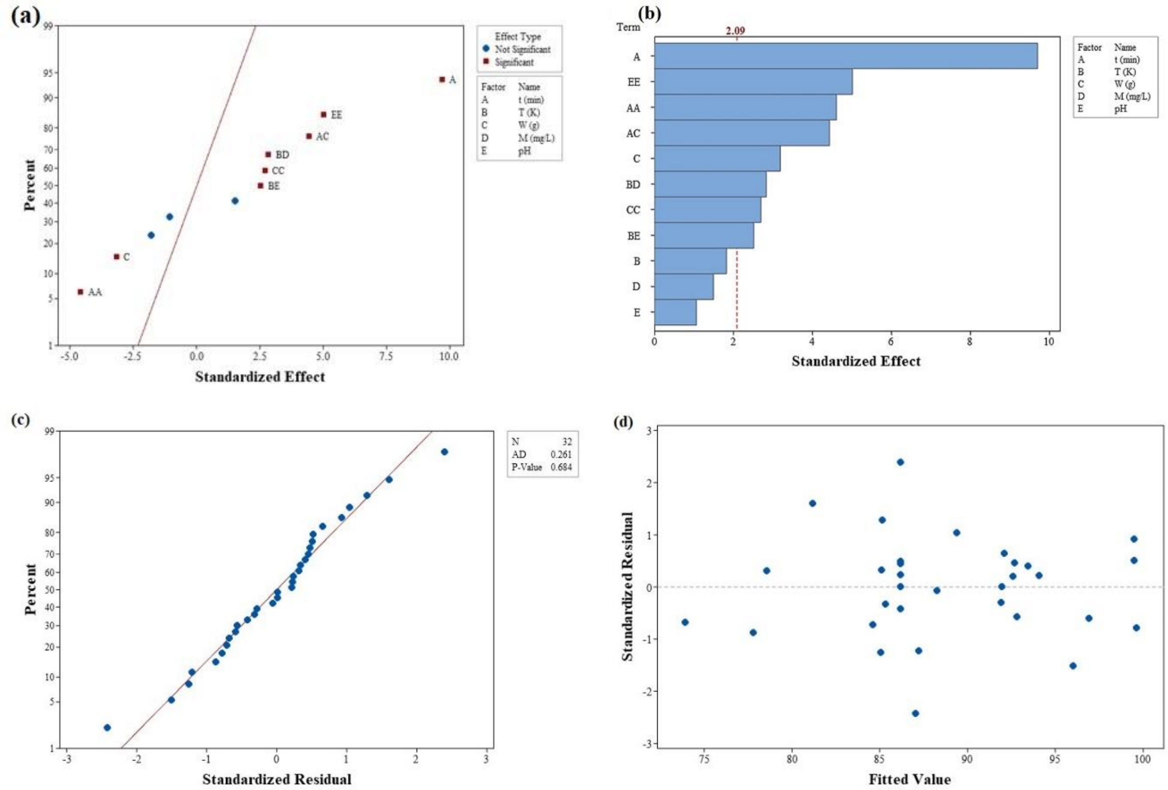

Figure 1: Diagnostic charts for Pb (II) ion removal onto POPP adsorbent based on the reduced model

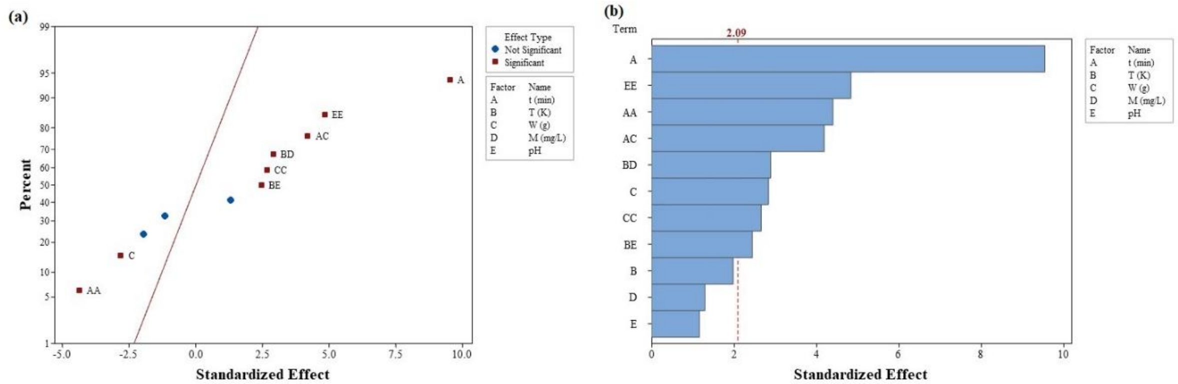

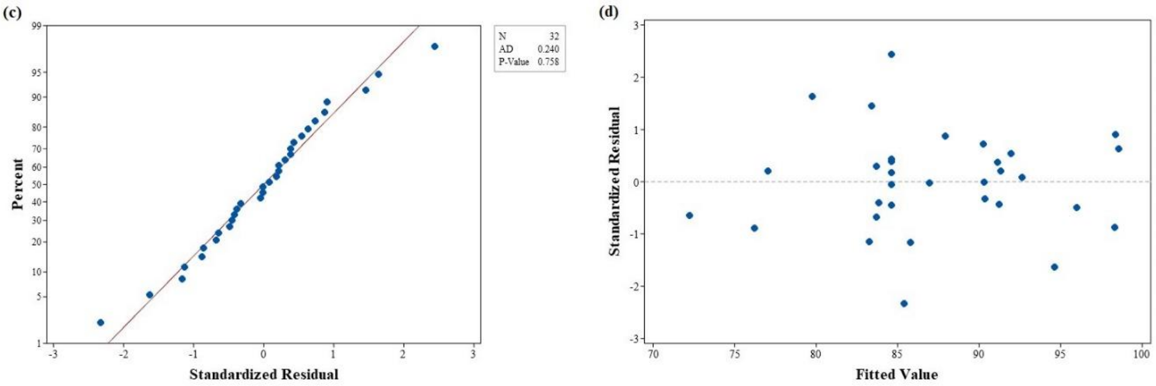

Figure 2: Diagnostic charts for Pb (II) ion removal onto AMPP adsorbent based on the reduced model

Influence of independent variables on responses

The three-dimensional (3D) response surface and two-dimensional (2D) contour plots for adsorption efficiencies of Pb (II) ions removal onto POPP and AMPP adsorbents versus the pairs of significant independent variables at the fixed mid values of all other variables are represented in Figure 3 and Figure 4, respectively. The presence of curvatures in the response surface and contour plots is characteristic of the interaction existing between any two independent variables affecting the adsorption process.

Effects of contact time and adsorbent weight

Figure 3(a) and Figure 3(b) present the interaction of contact time (X_1) and adsorbent weight (X_3) for removal onto POPP. The maximum Pb (II) ions adsorption is obtained at contact times of between 70-130 min. The initial adsorption rate at 30-70 min proceeded rapidly signifying that the relatively high surface area resulting from the abundant vacant active site on the adsorbent surface at the earlier stages of the Pb (II) ions removal process. More than 82.0% of Pb (II) ions could be removed by the adsorbent in the first 30 min before reaching equilibrium after 70 min of adsorption with desorption of the ions from the adsorbent setting in after about 138 min of adsorption has elapsed. The adsorption efficiency of POPP in the response surface and contour plots have been demonstrated to increase significantly (>82.5-90.0%) with an increase in the adsorbent weight (1.0-1.5 g) resulting from improved surface area occasioned by the increase in the number of vacant active sites, whereas it decreases slowly (>90.0-82.5%) at lower levels of the adsorbent amount (0.5-1.0 g) due to the high value of Pb (II) ions/vacant active sites ratio.

Effect of initial concentration

The effect of Pb (II) ions initial concentration (X_4) on its adsorption efficiency and its interaction with adsorption temperature are shown in Figure 3(c) and Figure 3(d). It is observed that the amount of Pb (II) ions uptake increase both at lower and higher initial concentration levels (10-500mg/L), indicating that the saturation point of the vacant sites on the adsorbent has not been reached by the concentration range. In other words, the ratio of Pb (II) ions concentration/vacant active sites on the POPP adsorbent is always low within the concentration profile leading to an increase in Pb (II) ions removal efficiency.

Effect of adsorbate pH

The interaction of adsorbate pH (X_5) with adsorption temperature is illustrated in Figure 3(e) and Figure 3(f). A decrease in adsorption efficiency of Pb (II) ions is observed with an increase in pH value (pH 3-6) and then increases steeply (pH 6-9). This is probably due to the high degree of protonation of the functional groups of the POPP adsorbent surface at low initial pH that favours the development of positive charge creating strong electrostatic repulsion between the cationic Pb (II) ions in the adsorbate and the adsorbent surface resulting in the significant decrease in adsorption efficiency. Whereas at a high degree of deprotonation of the functional groups of the POPP adsorbent surface taking place at high initial pH favours the development of negative charges leading to the strong electrostatic attraction between the cationic Pb (II) ions in the adsorbate and the adsorbent surface that causes a significant increase in adsorption efficiency. In other words, increasing the initial pH leads to the deprotonation of the adsorption sites (OH and COOH) and Pb (II) ions adsorption via electrostatic interaction as well as hydrogen bonding.

Effect of adsorption temperature

The interactions of adsorption temperature (X_2) with adsorbate concentration and adsorbate pH are illustrated in Figure 3(c) and Figure 3(e) for response surface and Figure 3(d) and Figure 3(f) for contour plots, respectively. As can be observed, this variable has a negative effect on the response, indicating that the higher the temperature, the lower the efficiency for Pb (II) ions removal onto the adsorbent. This trend conforms with the adsorption theory which affirms that adsorption efficiency decreases with increase in temperature whereas the earlier adsorbed species onto the adsorbent surface exhibit a greater tendency of desorbing from it at elevated temperatures. A temperature rise also increases the solute-solvent interaction forces as well as the solubility of the Pb (II) ions species in the wastewater medium, thereby bringing more difficulty in the adsorption process.

The trends observed in the response surface and contour plots for adsorption onto AMPP adsorbent (illustrated in Figure 4(a)-(f)) regarding the effects of all the predictor factors studied on the Pb (II) ions removal efficiency are quite similar to those described for adsorption onto POPP adsorbent discussed.

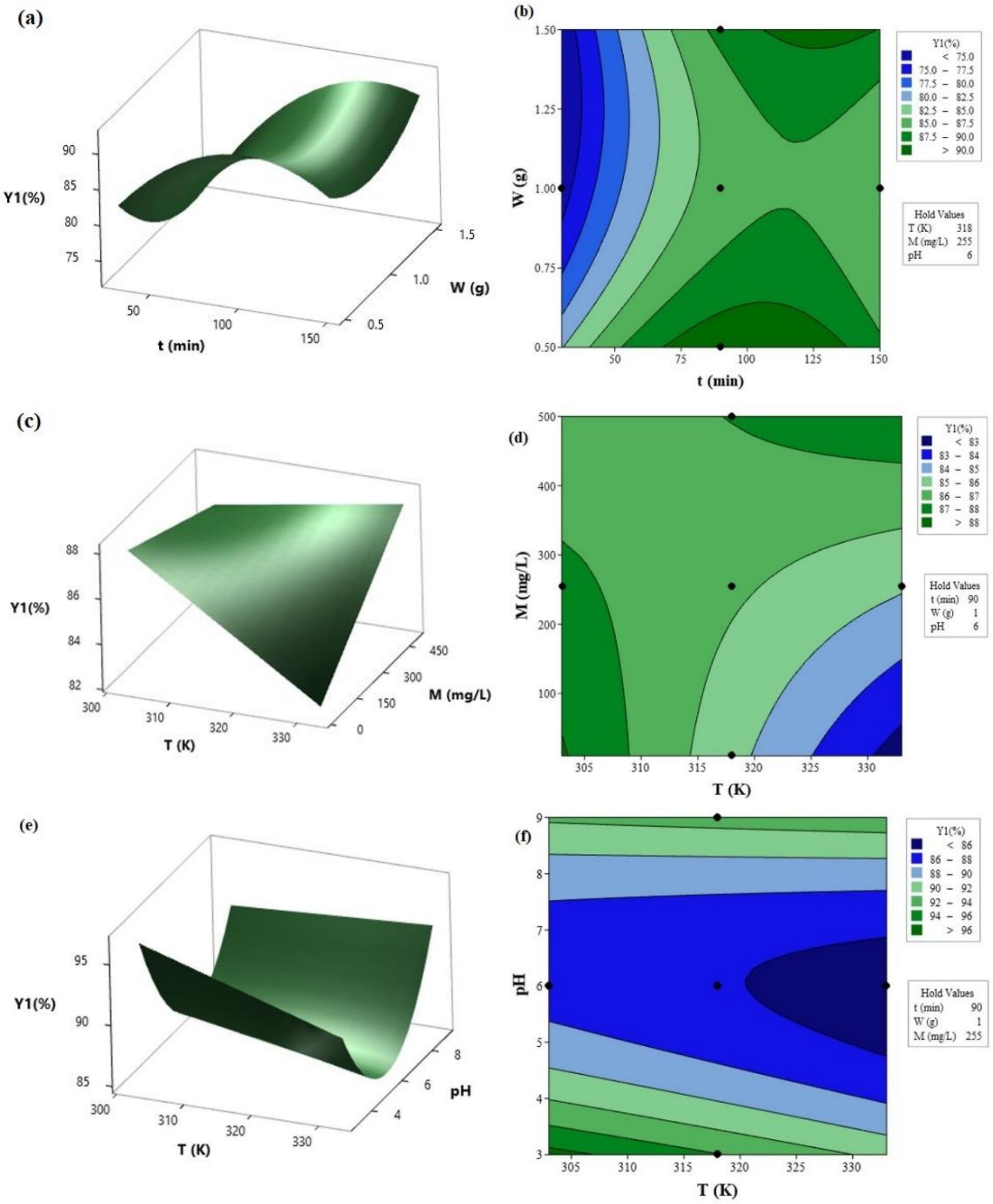

Figure 3: Response surface and contour plots for Pb (II) ion removal onto POPP adsorbent

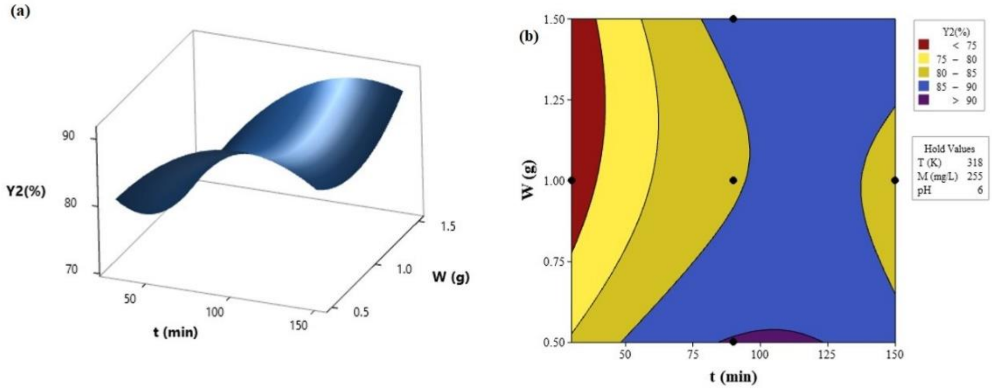

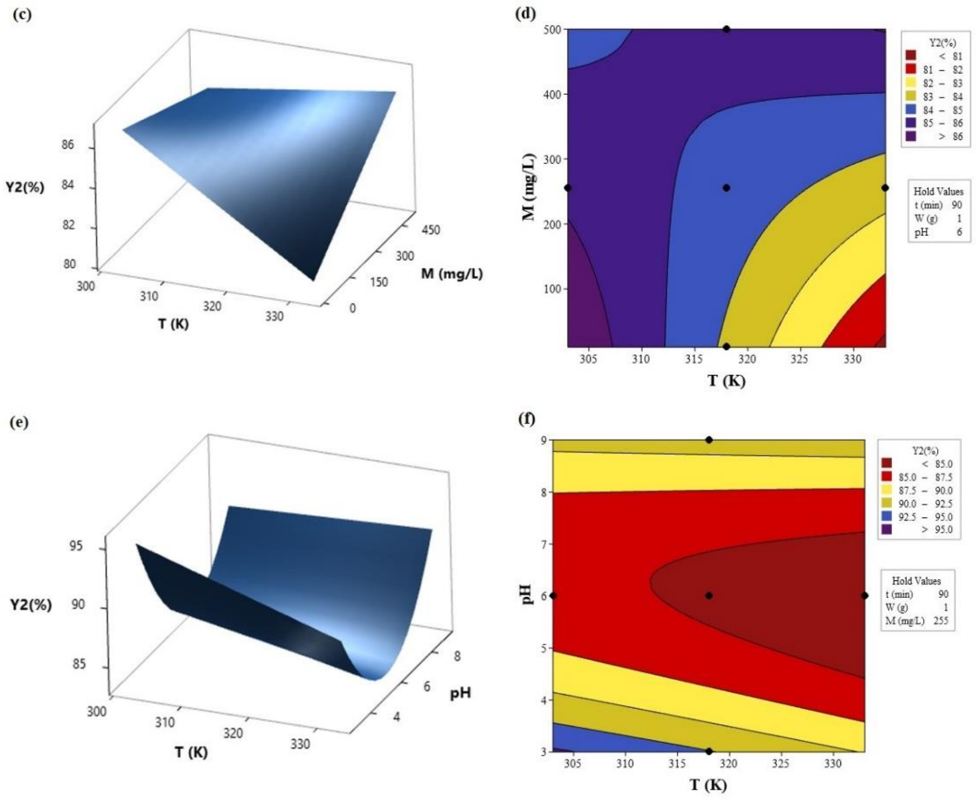

Figure 4: Response surface and contour plots for Pb (II) ion removal onto AMPP adsorbent

Optimization and validation of Pb (II) ions removal

The adsorption efficiencies for the removal of Pb (II) ions onto the two adsorbents were considered in this study with the central goal of maximizing the responses. A response optimizer tool that predicts the best set or sets of predictor variables operating based on composite desirability (*D*) and individual desirability (*d*) functions has been utilized to achieve the set goal. In this approach, controllable settings of the significant and hierarchical factors in the response surface design enable the achievement of a targeted, minimum, or maximum response desired. Better optimality of an optimization process is said to be attained when the values of the desirability functions (*D* or *d*) are equal to or close to one. As shown in Figure 5(a) and 5(b), the set of factors [X_1: 90 min, X_2: 318 °C, X_3: 0.5 g, X_4: 500 mg/L, X_5: 3.0] and [X_1: 90 min, X_2: 304 °C, X_3: 0.5 g, X_4: 500 mg/L, X_5: 3.0] provided the ideal settings of contact time, temperature, adsorbent weight, adsorbate concentration and a pH that achieved 100.7% and 100.0% removal of Pb (II) ions onto POPP and AMPP adsorbents with composite desirability values of one, respectively.

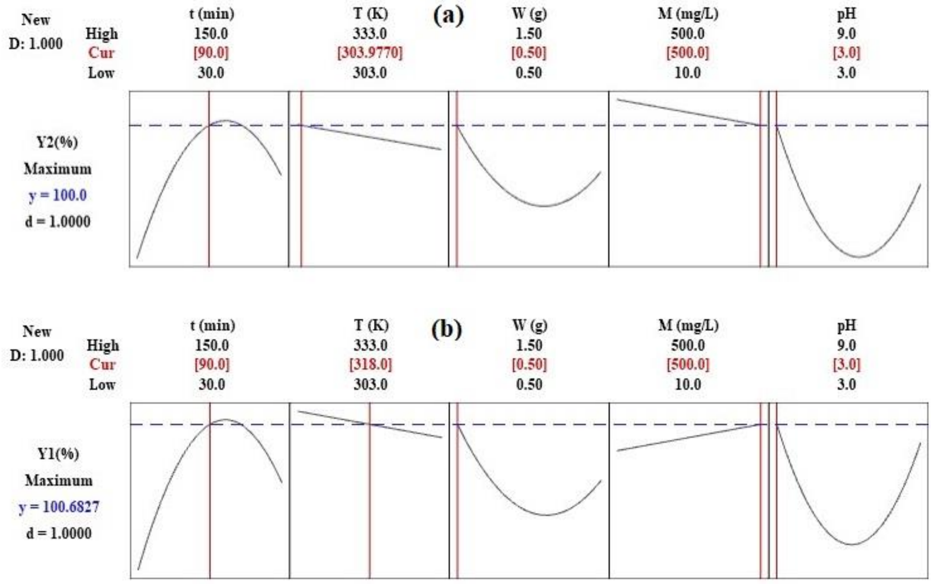

Figure 5: Optimizer plot for Pb (II) ion removal onto AMPP (a) and POPP (b) adsorbents

To verify the efficiency of the Minitab software in predicting the optimal values of the predictor variables during the optimization process, a set of five replicate experimental runs was carried out under the conditions predicted by the response optimizer tool. The mean Pb (II) ions removal efficiencies were found to be $99.8 \pm 0.9\%$ on POPP adsorbent and $98.1 \pm 0.9\%$ onto AMPP adsorbent. The variations in the experimentally observed responses and those predicted by the response optimizer were relatively negligible and thus insignificant. This suggested that the optimum set of the five factors supplied by the response optimizer are suitable for the total removal of the Pb (II) ions onto both adsorbents from the simulated wastewater samples.

CONCLUSION

The outcomes of this research work indicated that orange peels, in both its pristine and modified powder forms, have high adsorption efficiencies for the removal of lead (II) ions from simulated wastewater samples. Of all the significant terms in the RSM models, the contact time has been noticed to be the most prominent parameter followed by the quadratic term of the adsorbate pH while the interaction term of temperature and pH was identified to have the least prominence. Most of the statistically significant terms including the contact time, the quadratic term of the adsorbent weight, the interaction terms of the adsorption temperature with adsorbate concentration and with adsorbate pH have been found to have a synergistic influence on the Pb (II) ions removal onto both adsorbents. However, the adsorbent weight and the quadratic terms of the contact time were established to have antagonistic effects on the removal efficiencies. The reduced RSM models could satisfactorily describe high adsorption efficiencies of both pristine and acid-modified orange peels powders for lead (II) ions removal from aqueous solution. The two adsorbents have strong potential in facilitating the development of a viable technology for effective treatment of water via the adsorption mechanism.

REFERENCES

Ali, H., Khan, E. & Ilahi, I. (2019). Environmental chemistry and ecotoxicology of hazardous heavy metals: Environmental persistence, toxicity, and bioaccumulation. *Journal of Chemistry*, *2019*(Cd). https://doi.org/10.1155/2019/6730305

Asiminicesei, D. M., Vasilachi, I. C. & Gavrilescu, M. (2020). Heavy metal contamination of medicinal plants and potential implications on human health. *Revista de Chimie*, *71*(7), 16–36. https://doi.org/10.37358/RC.20.7.8222

Basu, M., Guha, A. K. & Ray, L. (2017). Adsorption of Lead on Cucumber Peel. *Journal of Cleaner Production*, *151*, 603–615. https://doi.org/https://doi.org/10.1016/j.jclepro.2017.03.028

Ben Khalifa, E., Rzig, B., Chakroun, R., Nouagui, H. & Hamrouni, B. (2019). Application of response surface methodology for chromium removal by adsorption on low-cost biosorbent. *Chemometrics and Intelligent Laboratory Systems*, *189*(April), 18–26. https://doi.org/10.1016/j.chemolab.2019.03.014

Blöcher, C., Dorda, J., Mavrov, V., Chmiel, H., Lazaridis, N. K. & Matis, K. A. (2003). Hybrid flotation - Membrane filtration process for the removal of heavy metal ions from wastewater. *Water Research*, *37*(16), 4018–4026. https://doi.org/10.1016/S0043-1354(03)00314-2

Duru, C., Ibrahim, F. B. & Dandajeh, A. A. (2023). Waste lemon peel as a circular solution for the remediation of lead-contaminated sludge for land application. *FUDMA Journal of Sciences*, *7*(6). https://doi.org/10.33003/fjs-2023-0706-2124

El-Naggar, I. M., Ahmed, S. A., Shehata, N., Sheneshen, E. S., Fathy, M. & Shehata, A. (2019). A novel approach for the removal of lead (II) ion from wastewater using Kaolinite/Smectite natural composite adsorbent. *Applied Water Science*, *9*(1), 1–13. https://doi.org/10.1007/s13201-018-0845-0

Gopinath, A., Krishna, K. & Karthik, C. (2020). Adsorptive Removal and Recovery of Heavy Metal Ions from Aqueous Solution/Effluents Using Conventional and Non-conventional Materials. *Modern Age Waste Water Problems*, 309–328. https://doi.org/10.1007/978-3-030-08283-3_15

Gunarathne, V., Ashiq, A. & Ginige, M. P. (2018). *Green Adsorbents for Pollutant Removal* (Vol. 18, Issue May). https://doi.org/10.1007/978-3-319-92111-2

Hameed, B. H., Mahmoud, D. K. & Ahmad, A. L. (2008). Sorption of basic dye from aqueous solution by pomelo (Citrus grandis) peel in a batch system. *Colloids and Surfaces A: Physicochemical and Engineering Aspects*, *316*(1–3), 78–84. https://doi.org/10.1016/j.colsurfa.2007.08.033

Heffron, J., Marhefke, M. & Mayer, B. K. (2016). Removal of trace metal contaminants from potable water by electrocoagulation. *Scientific Reports*, *6*(March), 1–9. https://doi.org/10.1038/srep28478

Ibrahim, Y., Abdulkarem, E., Naddeo, V., Banat, F. & Hasan, S. W. (2019). Synthesis of super hydrophilic cellulose-alpha zirconium phosphate ion exchange membrane via surface coating for the removal of heavy metals from wastewater. *Science of the Total Environment*, *690*, 167–180. https://doi.org/10.1016/j.scitotenv.2019.07.009

Ighalo, J. O. & Adeniyi, A. G. (2020). Adsorption of pollutants by plant bark derived adsorbents: An empirical review. *Journal of Water Process Engineering*, *35*(February), 101228. https://doi.org/10.1016/j.jwpe.2020.101228

Igwe, J. C., Onyegbado, C. O. & Abia, A. A. (2010). Adsorption isotherm studies of BOD, TSS and colour reduction from palm oil mill effluent (POME) using boiler fly ash. *Eclética Química*, *35*(3), 195–208. https://doi.org/10.1590/s0100-46702010000300020

Iloms, E., Ololade, O. O., Ogola, H. J. O. & Selvarajan, R. (2020). Investigating industrial effluent impact on municipal wastewater treatment plant in vaal, South Africa. *International Journal of Environmental Research and Public Health*, *17*(3), 1–18. https://doi.org/10.3390/ijerph17031096

Joshi, S., Kataria, N., Garg, V. K. & Kadirvelu, K. (2020). Pb2+ and Cd2+ recovery from water using residual tea waste and SiO2@TW nanocomposites. *Chemosphere*, *257*, 127277. https://doi.org/https://doi.org/10.1016/j.chemosphere.2020.127277

Knoema. (2018). *Nigeria - Citrus fruit production quantity*. World Atlas. https://knoema.com/atlas/Nigeria/topics/Agriculture/Crops-%0AProduction-Quantity-tonnes/Citrus-fruit-production.

Li, W., Zhang, L., Peng, J., Li, N., Zhang, S. & Guo, S. (2008). Tobacco stems as a low cost adsorbent for the removal of Pb(II) from wastewater: Equilibrium and kinetic studies. *Industrial Crops and Products*, *28*(3), 294–302. https://doi.org/10.1016/j.indcrop.2008.03.007

Liu, Y. & Ma, R. (2020). Human health risk assessment of heavy metals in groundwater in the luan river catchment within the North China Plain. *Geofluids*, *2020*. https://doi.org/10.1155/2020/8391793

Minitab®. (2019). *Minitab® statistical software version 19.1 for Windows (64-bit)*. Minitab, LLC, the United States and Other Countries. https://www.minitab.com

Moyo, M., Chikazaza, L., Nyamunda, B. C. & Guyo, U. (2013). Adsorption batch studies on the removal of Pb(II) using maize tassel based activated carbon. *Journal of Chemistry*, *2013*. https://doi.org/10.1155/2013/508934

Petrinic, I., Korenak, J., Povodnik, D. & Hélix-Nielsen, C. (2015). A feasibility study of ultrafiltration/reverse osmosis (UF/RO)-based wastewater treatment and reuse in the metal finishing industry. *Journal of Cleaner Production*, *101*, 292–300. https://doi.org/10.1016/j.jclepro.2015.04.022

Raril, C. & Manjunatha, J. G. (2020). Fabrication of novel polymer-modified graphene-based electrochemical sensor for the determination of mercury and lead ions in water and biological samples. *Journal of Analytical Science and Technology*, *11*(1). https://doi.org/10.1186/s40543-019-0194-0

Sani, S., Abdullahi, H. & Mazoji, A. M. (2019). Screening experimental design for adsorption of lead (II) Ions from modelled effluent onto raw and functionalized orange peels. *Records of Chemical Sciences*, *1*(3), 86–101.

Soo, K. W., Wong, K. C., Goh, P. S., Ismail, A. F. & Othman, N. (2020). Efficient heavy metal removal by thin film nanocomposite forward osmosis membrane modified with geometrically different bimetallic oxide. *Journal of Water Process Engineering*, *38*(August), 101591. https://doi.org/10.1016/j.jwpe.2020.101591

Tunali Akar, S., Arslan, S., Alp, T., Arslan, D. & Akar, T. (2012). Biosorption potential of the waste biomaterial obtained from Cucumis melo for the removal of Pb 2+ ions from aqueous media: Equilibrium, kinetic, thermodynamic and mechanism analysis. *Chemical Engineering Journal*, *185–186*, 82–90. https://doi.org/10.1016/j.cej.2012.01.032

Ungureanu, O. I., Bulgariu, D., Mocanu, A. M. & Bulgariu, L. (2020). Functionalized PET waste based low-cost adsorbents for adsorptive removal of Cu(II) ions from aqueous media. *Water (Switzerland)*, *12*(9), 1–12. https://doi.org/10.3390/W12092624

World Health Organization. (2011). *Lead in drinking water: Background document for development of WHO Guidelines for drinking-water quality*. 1–19. https://doi.org/10.2105/ajph.13.3.207

Wu, H., Huang, Y., Liu, B., Han, G., Su, S., Wang, W., Yang, S., Xue, Y. & Li, S. (2021). An efficient separation for metal-ions from wastewater by ion precipitate flotation: Probing formation and growth evolution of metal-reagent flocs. *Chemosphere*, *263*, 128363. https://doi.org/10.1016/j.chemosphere.2020.128363

Wu, J., Wang, T., Wang, J., Zhang, Y. & Pan, W. P. (2021). A novel modified method for the efficient removal of Pb and Cd from wastewater by biochar: Enhanced the ion exchange and precipitation capacity. *Science of the Total Environment*, *754*, 142150. https://doi.org/10.1016/j.scitotenv.2020.142150

Zhou, N., Chen, H., Feng, Q., Yao, D., Chen, H., Wang, H., Zhou, Z., Li, H., Tian, Y. & Lu, X. (2017). Effect of phosphoric acid on the surface properties and Pb(II) adsorption mechanisms of hydrochars prepared from fresh banana peels. *Journal of Cleaner Production*, *165*, 221–230. https://doi.org/https://doi.org/10.1016/j.jclepro.2017.07.111

Zhou, N., Chen, H., Xi, J., Yao, D., Zhou, Z., Tian, Y. & Lu, X. (2017). Biochars with excellent Pb(II) adsorption property produced from fresh and dehydrated banana peels via hydrothermal carbonization. *Bioresource Technology*, *232*, 204–210. https://doi.org/https://doi.org/10.1016/j.biortech.2017.01.074